

# Resolution of sub-wavelength lenses formed by the wire medium

Pavel A. Belov

*Department of Electronic Engineering, Queen Mary University of London,  
Mile End Road, London, E1 4NS, United Kingdom*

Mário G. Silveirinha

*Departamento de Eng. Electrotécnica da Universidade de Coimbra,  
Instituto de Telecomunicações, Pólo II, 3030 Coimbra, Portugal*

(Dated: February 9, 2020)

The restrictions on the resolution of the lenses formed by wire media (square arrays of conductive cylinders) recently proposed in [Phys. Rev. B, 71, 193105 (2005)] are studied in this paper. It is demonstrated, using both analytical and numerical modeling, that the lenses have sub-wavelength resolution that can in principle be made as fine as required for a certain application by controlling the lattice constant of the wire medium. This confirms that the lenses formed by wire medium are unique imaging devices capable of transmitting distributions of TM-polarized electric fields with nearly unlimited sub-wavelength resolution at the microwave frequency range.

PACS numbers: 78.20.Ci, 42.70.Qs, 42.25.Fx, 73.20.Mf

## I. INTRODUCTION

Recently a new type of lenses with sub-wavelength resolution was suggested in [1]. These lenses are formed by planar slabs of materials with specific electromagnetic properties, and operate as transmission devices that are able to transfer an image from one plane to another with sub-wavelength resolution. Such regime of operation is called canalization. In order to implement the canalization regime it is required to use materials in which the electromagnetic waves have a flat isofrequency contour. These media are capable of transmitting energy only in one direction, always with the same phase speed. The typical example of such materials is the wire medium (see Fig. 1), which consists of an array of parallel ideally conducting wires [2, 3, 4, 5] operating at frequencies smaller than its characteristic plasma frequency.

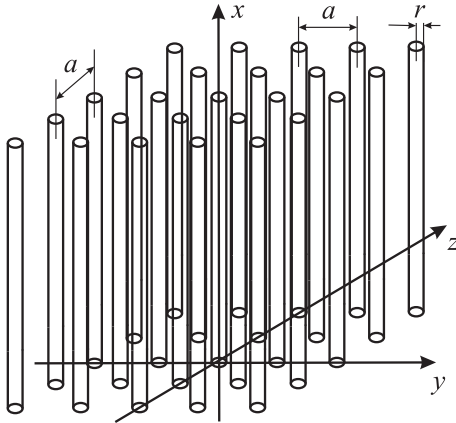


FIG. 1: The geometry of the wire medium: a square lattice of parallel ideally conducting thin wires.

The wire medium supports transmission line modes which travel along the wires at the speed of light. A

slab of wire medium with thickness equal to an integer number of half-wavelengths experiences Fabry-Perot resonance for any angle of incidence, including complex ones, and thus such a slab is capable of transporting images with sub-wavelength resolution [6]. The lenses formed by wire medium were studied both numerically and experimentally in [6]. As result, the imaging with  $\lambda/15$  resolution has been successfully demonstrated. In [6] it was assumed that the lens operates at a very low frequency as compared to its plasma frequency and no estimation has been made on how the plasma-like properties of the wire medium could affect the operation of such lenses. In order to reveal the restrictions on the resolution of the sub-wavelength lenses caused by plasma-like properties of the wire medium, in the present paper we theoretically study the transmission through a wire medium slab using the results recently obtained in [7]. The theoretical results are validated by numerical modeling using the periodic method of moments [8].

## II. WIRE MEDIUM

The wire medium is a material characterized by strong spatial dispersion even at low frequencies [5]. It can be described by a spatially dispersive permittivity tensor of the form,

$$\bar{\epsilon} = \epsilon \mathbf{xx} + \mathbf{yy} + \mathbf{zz}, \quad \epsilon(\omega, q_x) = 1 - \frac{k_p^2}{k^2 - q_x^2}, \quad \text{leff} \quad (1)$$

where the  $x$ -axis is oriented along wires,  $q_x$  is the  $x$ -component of wave vector  $\mathbf{q}$ ,  $k = \omega/c$  is the wave number of the host medium,  $c$  is the speed of light, and  $k_p = \omega_p/c$  is the wave number corresponding to the plasma frequency  $\omega_p$ . The plasma frequency depends on the lattice

period  $a$  and on the radius of wires  $r$  [9]:

$$k_p^2 = \frac{2\pi/a^2}{\ln \frac{a}{2\pi r} + 0.5275} \cdot lk_0 \quad (2)$$

Note that in this paper we assume that the metallic wires are arranged in a square lattice. The permittivity tensor is normalized to the permittivity of the host medium.

The solution of any boundary problem involving the wire medium (using an effective medium theory) requires the knowledge of an additional boundary condition at the interface. In fact, it has long been known that the usual boundary conditions (continuity of the tangential components of the electromagnetic field) are insufficient in case of spatial dispersion [10, 11, 12]. Such an additional boundary condition has been formulated in [7] for the wire medium case. It was proved that the normal component of the electric field must be continuous at the interface between the wire medium and free space, under the condition that the host medium of the wire medium is also free space. In this paper, we will use this result to study the resolution of the wire medium lens. Firstly, in the next section we characterize the scattering of plane waves by a wire medium slab.

### III. REFLECTION COEFFICIENT FOR A WIRE MEDIUM SLAB

Let us consider a slab of wire medium with thickness  $d$  (see Fig. 2). We suppose that the wires stand in free-space and are normal to the interface. The wires are assumed perfectly conducting, i.e. losses are assumed negligible. As is well-known, an image at the input plane of the lens can be decomposed in terms of spatial harmonics. The spatial harmonics are either propagating plane waves or evanescent plane waves, and their polarization can be classified as transverse electric (TE) or transverse magnetic (TM) with respect to the orientation of the wires. In [6] it was proved that the wire medium lens allows sub-wavelength imaging of the part of the spectrum with TM-polarization.

To evaluate the resolution of the imaging, we consider that a plane wave with TM polarization impinges on the slab. Let  $H_{\text{inc}}$  be the amplitude of the incident magnetic field along the  $z$ -direction, and let  $\mathbf{k} = (k_x, k_y, 0)^T$  be the wave vector of the incident wave. The  $x$ -component of the wave vector  $k_x$  can be expressed in terms of the wave number  $k$  and of the  $y$ -component of the wave vector  $k_y$  as  $k_x = -j\sqrt{k_y^2 - k^2}$ . The incident plane wave excites two types of waves in the wire medium: the extraordinary wave (TM mode) and the transmission line (TEM) mode [5]. The ordinary wave is not excited since it has TE polarization. The tangential component of the wave vector  $k_y$  is conserved at the interface between free space and the wire medium. Using this property we can evaluate the wave vector associated with each of the excited modes in the slab. The wave vector associated with

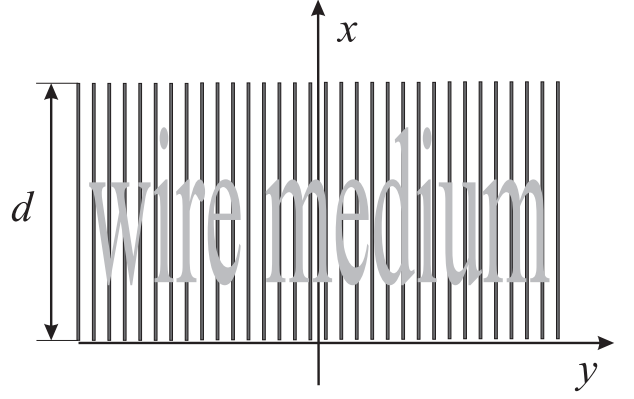


FIG. 2: The wire medium slab. The structure is unbounded and periodic along the  $y$ - and  $z$ -directions.

transmission line modes is of the form:

$$\mathbf{q}_{\pm}^{\text{TEM}} = (\pm k, k_y, 0)^T. \quad (3)$$

These waves travel along the wires with the speed of light in free space, independently of the value of transverse component of wave vector  $k_y$ . On the other hand, the extraordinary modes obey to the dispersion equation derived in [5],

$$q_x^2 + q_y^2 + q_z^2 = k^2 - k_p^2. \quad (4)$$

and thus the wave vector of an extraordinary mode is of the form:

$$\mathbf{q}_{\pm}^{\text{TM}} = (\pm q_x, k_y, 0), \quad q_x = -j\sqrt{k_p^2 + k_y^2 - k^2}. \quad (5)$$

If the frequency of operation is smaller than the plasma frequency ( $k < k_p$ ), then the extraordinary modes are evanescent: the  $x$ -component of wave vector  $q_x$  is a purely imaginary number for any real  $k_y$ . In order to emphasize this it is convenient to use the notation  $q_x = -j\gamma_{\text{TM}}$  with  $\gamma_{\text{TM}} = \sqrt{k_p^2 + k_y^2 - k^2}$ . Also, by analogy, we denote  $k_x = -j\gamma_x$  with  $\gamma_x = \sqrt{k_y^2 - k^2}$ . The value of  $\gamma_x$  is purely imaginary if  $k_y < k$  (propagating modes in free space), but it becomes a real number if  $k_y > k$  (evanescent modes in free space, i.e. the sub-wavelength spatial spectrum).

The total magnetic field (directed along the  $z$ -axis) can be written in the following form:

$$\frac{H(x)}{H_{\text{inc}}} = \begin{cases} e^{-jk_x x} + R e^{jk_x x}, & x < 0 \\ A_{-}^{\text{TM}} e^{-\gamma_{\text{TM}}(x-d/2)} + A_{+}^{\text{TM}} e^{+\gamma_{\text{TM}}(x-d/2)} + A_{-}^{\text{TEM}} e^{-jk(x-d/2)} + A_{+}^{\text{TEM}} e^{+jk(x-d/2)}, & 0 \leq x \leq d \\ T e^{-jk_x(x-d)}, & x > d, \end{cases} \quad (6)$$

where  $R$  and  $T$  are the reflection and transmission coefficients,  $A_{\pm}^{\text{TM}}$  and  $A_{\pm}^{\text{TEM}}$  are the amplitudes the extraordinary (TM) and transmission-line (TEM) modes in the slab, respectively.

Following [7], all components of both magnetic and electric fields are continuous at the interface between free space and the wire medium. Thus, the magnetic field  $H(x)$  and both its first  $dH(x)/dx$  and second

$d^2H(x)/dx^2$  derivatives by  $x$  are continuous at interfaces  $x = 0$  and  $x = d$ . This can be written using  $\vec{H}$  in the form of the following system of equations:

$$\begin{pmatrix} -1 & e^{\gamma_{\text{TM}}d/2} & e^{-\gamma_{\text{TM}}d/2} & e^{jkd/2} & e^{-jkd/2} & 0 \\ -jk_x & -\gamma_{\text{TM}}e^{\gamma_{\text{TM}}d/2} & \gamma_{\text{TM}}e^{-\gamma_{\text{TM}}d/2} & -jke^{jkd/2} & jke^{-jkd/2} & 0 \\ k_x^2 & \gamma_{\text{TM}}^2e^{\gamma_{\text{TM}}d/2} & \gamma_{\text{TM}}^2e^{-\gamma_{\text{TM}}d/2} & -k^2e^{jkd/2} & -k^2e^{-jkd/2} & 0 \\ 0 & e^{-\gamma_{\text{TM}}d/2} & e^{\gamma_{\text{TM}}d/2} & e^{-jkd/2} & e^{jkd/2} & -1 \\ 0 & -\gamma_{\text{TM}}e^{-\gamma_{\text{TM}}d/2} & \gamma_{\text{TM}}e^{\gamma_{\text{TM}}d/2} & -jke^{-jkd/2} & jke^{jkd/2} & jk_x \\ 0 & \gamma_{\text{TM}}^2e^{-\gamma_{\text{TM}}d/2} & \gamma_{\text{TM}}^2e^{\gamma_{\text{TM}}d/2} & -k^2e^{-jkd/2} & -k^2e^{jkd/2} & k_x^2 \end{pmatrix} \begin{pmatrix} R \\ A_{-}^{\text{TM}} \\ A_{+}^{\text{TM}} \\ A_{-}^{\text{TEM}} \\ A_{+}^{\text{TEM}} \\ T \end{pmatrix} = \begin{pmatrix} 1 \\ -jk_x \\ -k_x^2 \\ 0 \\ 0 \\ 0 \end{pmatrix} \quad (7)$$

Solving this system the transmission coefficient  $T$  can be expressed as follows:

$$T = \frac{1}{1 + \frac{\gamma_{\text{TM}}k_y^2}{\gamma_x(k_y^2 + k_p^2)} \tanh(\gamma_{\text{TM}}d/2) - \frac{kk_p^2}{\gamma_x(k_y^2 + k_p^2)} \tan(kd/2)} - \frac{1}{1 + \frac{\gamma_{\text{TM}}k_y^2}{\gamma_x(k_y^2 + k_p^2)} \text{ctanh}(\gamma_{\text{TM}}d/2) + \frac{kk_p^2}{\gamma_x(k_y^2 + k_p^2)} \text{ctan}(kd/2)} \cdot lT \quad (8)$$

In the above "tanh" and "ctanh" represent the hyperbolic tangent and cotangent, respectively. The canalization regime is observed for the slab under consideration when  $kd = n\pi$ , where  $n$  is an integer. In this case  $T$  can be simplified: if  $kd = (2n+1)\pi$  then

$$T = -\frac{1}{1 + \frac{\gamma_{\text{TM}}k_y^2}{\gamma_x(k_y^2 + k_p^2)} \text{ctanh}(\gamma_{\text{TM}}d/2)}, l_{2n1} \quad (9)$$

whereas if  $kd = 2n\pi$  then

$$T = \frac{1}{1 + \frac{\gamma_{\text{TM}}k_y^2}{\gamma_x(k_y^2 + k_p^2)} \tanh(\gamma_{\text{TM}}d/2)}, l_{2n} \quad (10)$$

The transmission coefficient calculated above can be regarded as a transfer function: the image at the output plane is obtained by superimposing the (TM-polarized) spatial harmonics of the source field distribution at the input plane multiplied by  $T$ . Strictly speaking, that is not rigorously true, even if the exact expression for transmission coefficient is known. Indeed, when doing this we are neglecting the higher order harmonics, which decay much faster than the fundamental mode, but also contribute to the near field. These harmonics are a manifestation of the actual granularity of wire medium, and are not described by the effective medium model eff. The contribution of the high order harmonics can be neglected while  $k_y a < \pi$ , which corresponds to operation below the ultimate limiting resolution  $\Delta/2 = a$  [13]. In this case, slight variations of the near field near the edges of the

wires do not influence the resolution of the lens. Thus, in this paper we will consider that the distribution of the field at the output plane is equal to the distribution of the field at the input plane multiplied by the transmission coefficient. Within this approximation, it is sufficient to characterize  $T$  in order to evaluate the resolution of the lens.

If the operating frequency is much smaller than the plasma frequency, i.e.  $k \ll k_p$ , then since  $kd/\pi > 1$  we can assume that  $\gamma_{\text{TM}}d \gg 1$ , and using the expressions  $\text{t2n1}$  and  $\text{t2n}$  we obtain a simple approximate formula for transmission coefficient:

$$T \approx \mp \frac{1}{1 + \frac{\gamma_{\text{TM}}k_y^2}{\gamma_x(k_y^2 + k_p^2)}}, l_{app} \quad (11)$$

where the  $\mp$  sign corresponds to the case in which the thickness of the slab is equal to an even or odd number of half-wavelengths, respectively.

Some important properties of the formulae  $\text{t2n1}$  and  $\text{t2n}$  are readily identified. It is clear that if  $k_p \rightarrow \infty$  then  $T \approx \mp 1$  for any  $k_y$ , and therefore, in such conditions, the imaging is perfect for this polarization. On the other hand, one can see that  $T = 0$  when  $\gamma_x = 0$ . i.e.  $k_y = k$ . This property is very important because it shows that the spatial harmonics with  $k_y = k$  are filtered by the WM, which kind of contradicts the sub-wavelength imaging. Actually, as it will be demonstrated below, the band of the spatial harmonics corresponding to this filtering is so narrow that it practically does not affect the imaging properties of the system.

Also, it is clear that the imaging quality does not depend on the thickness of the lens. The lens can be made as thick as it may be required by an application. The only restriction is that the thickness has to be equal to an integer number of half-wavelengths. If the number of half-wavelengths is odd then the image at the back interface of the lens will appear out-of phase with respect to the source, whereas if the number of half-wavelengths is even then the image and the source will be in phase. Moreover, the bandwidth of operation does not depend

on the thickness of the lens. It remains the same for all slab thicknesses equal to the integer number of half-wavelengths.

#### IV. STUDY OF RESOLUTION

In [6] the wire medium with period  $a = 1\text{cm}$  formed by wires with  $r = 1\text{mm}$  has been considered. Substitution of these parameters into  $k_0$  gives  $k_p a = 2.5$  (a more accurate value, calculated numerically using the numerical method proposed in [14], is  $k_p a = 2.36$ ). The frequency of operation for the lens in [6] was  $1\text{GHz}$ , which corresponds to  $ka = 0.2$ . The thickness  $d$  of the lens in [6] was chosen to be equal to the half-wavelength, that is  $kd = \pi$ . In the present paper we consider the same parameters for the lens.

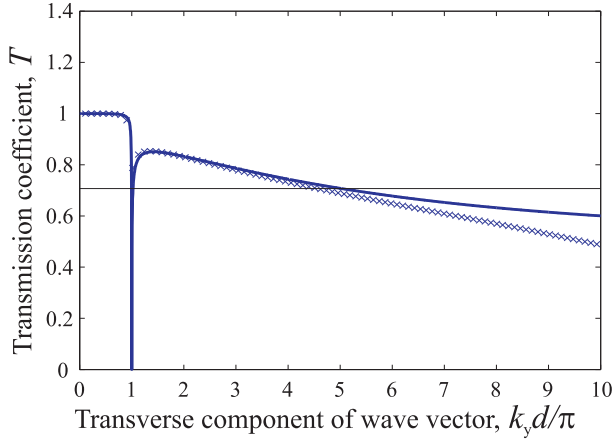


FIG. 3: Transmission coefficient  $T$  (absolute value) as a function of the transverse component of wave vector  $k_y d / \pi$  for  $k_p d / \pi = 11.3$  and  $kd / \pi = 1$ . Solid line: analytical model  $T$ . Crosses: points calculated with the full wave numerical method.

The dependence of the transmission coefficient (absolute value) on the normalized transverse component of wave vector  $k_y d / \pi$  is plotted in Fig. 3. One can see that the transmission coefficient has a very sharp dip at  $k_y = k$ , but for other values of  $k_y$  it has values close to unity. In Fig. 3 the "crosses" represent the data calculated numerically using the periodic method of moments. As seen, the agreement between the analytical model and the full wave results is very satisfactory. We do not present a plot for phase of transmission coefficient since it is practically equal to  $\pi$  for whole range of  $k_y$ , except for a very narrow band with upper bound equal to  $k$ . The obtained dependence confirms that the slab indeed operates in the canalization regime and is capable of transporting sub-wavelength images with TM polarization. In order to evaluate the resolution of this lens, we use the usual criterion of half-intensity: we assume that the imaging happens while the transmission coefficient of spatial harmonics is in the range  $[1/\sqrt{2}, \sqrt{2}]$ . For

the case presented in Fig. 3, the transmission coefficient  $T$  is less than 1 and greater than  $1/\sqrt{2}$  for  $k_y d / \pi < 5$  except for the very narrow range of  $k_y d / \pi$  close to 1. This means that the resolution of the lens under consideration is equal to  $\Delta/2 = \pi/k_y^{\max} = \lambda/10$ . This value is only three times larger than the ultimate limit of resolution due to periodicity of the structure  $\Delta_l/2 = a = \lambda/30$  formulated in [13], and a bit worse than the real resolution of  $2a = \lambda/15$  observed at [6].

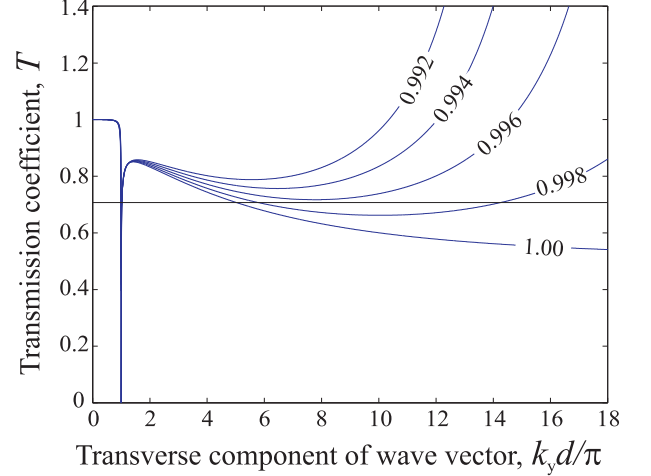


FIG. 4: Transmission coefficient  $T$  (absolute value) as a function of the transverse component of wave vector  $k_y d / \pi$  for  $k_p d / \pi = 11.3$  and  $kd / \pi = 1 - 0.002n$ , where  $n=0,1,2,3,4$ . The numbers at the figure correspond to the values of  $kd / \pi$ .

The reason of the discrepancy can be readily revealed if the frequency of operation is slightly changed. In Fig. 4, the transmission characteristic is depicted for frequencies that are lower than original frequency of operation by 0.2, 0.4, 0.6 and 0.8%. It is seen that the amplitude of the evanescent modes is amplified in a certain range of  $k_y$ . This helps to improve the resolution of the lens. For example, in the case of  $kd / \pi = 0.996$  the resolution happens to be equal to  $\lambda/34$  which is even smaller than the ultimate limit dictated by periodicity. This phenomenon can be one of the reasons why in the experiment described in [6] the resolution of  $\lambda/15$  has been observed at the frequency of 980MHz which is also slightly smaller than the frequency of design 1GHz.

The further decrease of the frequency of operation reveals a very interesting resonant phenomenon. This is illustrated in Fig. 5, where the transmission coefficient is plotted for frequencies which are lower than the design frequency by 1, 2, 3, 4, 5 and 6%. One can observe a very strong enhancement of certain spatial harmonics. This property reveals the presence of waveguiding modes propagating along the  $y$  direction of the slab, being the mechanism of propagation closely related to that of the wave that propagates in an Yagi antenna array [15].

The observed resonant enhancement destroys the sub-wavelength imaging since some of the spatial harmonics happen to be amplified by a factor of 10 or even more.

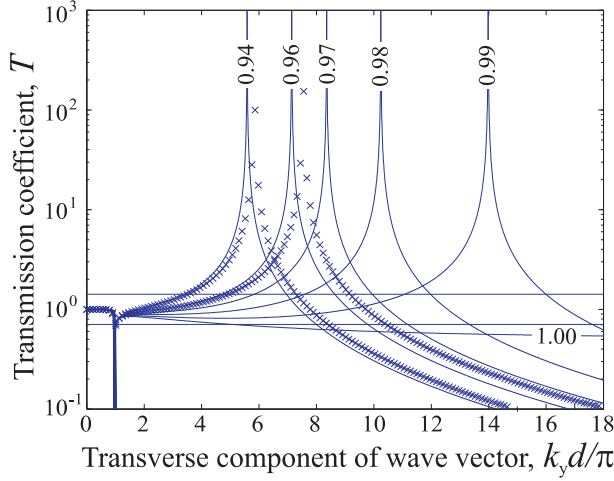


FIG. 5: Transmission coefficient  $T$  (absolute value) as a function of the transverse component of wave vector  $k_y d / \pi$  for  $k_p d / \pi = 11.3$  and  $kd / \pi = 1 - 0.01n$ , where  $n=0,1,2,3,4,6$ . The numbers in the figure correspond to the values of  $kd / \pi$ . The crosses represent the results of the numerical modeling for  $kd / \pi = 0.94$  and  $kd / \pi = 0.96$ .

When  $kd / \pi = 0.96$  the resolution is reduced down to  $\lambda / 10$ . One can see that imaging with a resolution better than  $\lambda / 10$  is observed for  $kd / \pi \in [0.96, 1.00]$ . This means that the bandwidth of operation with  $\lambda / 10$  or better resolution is equal to 4% for the lens under consideration. The bandwidth of imaging with worse but still sub-wavelength resolution can be even larger. In [6] the 15% bandwidth of imaging with sub-wavelength resolution has been reported.

For frequencies above the design frequency, the resolution of the lens is quickly deteriorated. This can be

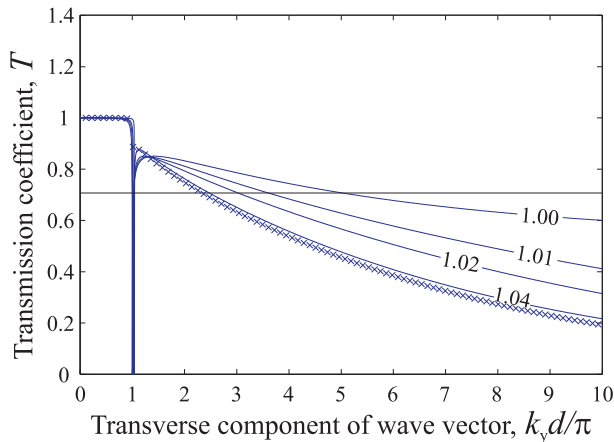


FIG. 6: Transmission coefficient  $T$  (absolute value) as a function of the transverse component of wave vector  $k_y d / \pi$  for  $k_p d / \pi = 11.3$  and  $kd / \pi = 1 + 0.01n$ , where  $n=0,1,2,4$ . The numbers at the figure correspond to the values of  $kd / \pi$ . The crosses represent the results of the numerical modeling for  $kd / \pi = 1.04$ .

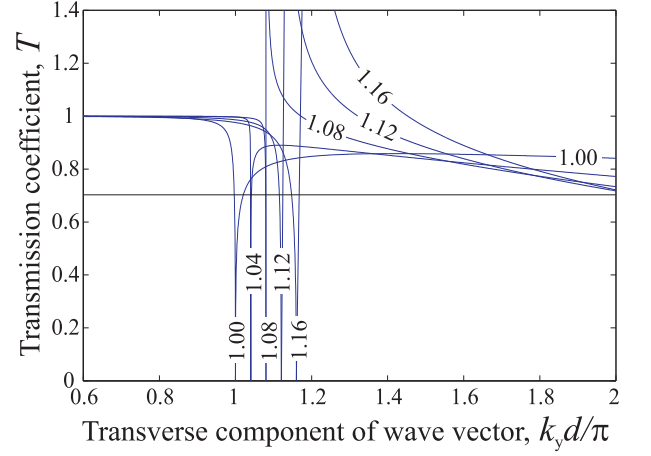


FIG. 7: Transmission coefficient  $T$  (absolute value) as a function of the transverse component of wave vector  $k_y d / \pi$  for  $k_p d / \pi = 11.3$  and  $kd / \pi = 1 + 0.04n$ , where  $n=0,1,2,3,4$ . The numbers in the figure correspond to the values of  $kd / \pi$ .

clearly seen from the Fig. 6, where the transmission coefficient is plotted for frequencies greater than the design frequency by 1, 2 and 4%. Moreover, the width of the narrow dip close to  $k_y = k$  increases and some resonant behavior appears. This effect is illustrated in Fig. 7 where the transmission characteristic is depicted for frequencies greater than design frequency by 4, 8, 12 and 16%.

## V. IMPROVEMENT OF RESOLUTION

We summarize our results for the dependence of the resolution  $\Delta / 2 = \pi / k_y^{\max}$  on the frequency in Fig. 8. By tuning the frequency one can dramatically enhance the resolution. In practice this means that it is always possible to reach an ultimate limiting resolution  $\Delta / 2 = a$  [13] by appropriately choosing the frequency of operation. The value of the resolution for the case  $kd / \pi = 1$  approximately describes an average level of resolution of the system.

From equation app it is clear that if  $k_y \gg k$  (deep sub-wavelength spatial spectrum) then

$$T \approx \mp \frac{1}{1 + \frac{k_y}{\sqrt{k_y^2 + k_p^2}}}. \quad (12)$$

This expression allows to evaluate resolution of the system  $\Delta / 2 = \pi / k_y^{\max}$  for the case then  $kd / \pi = 1$ . Solving the equation  $T(k_y^{\max}) = 1 / \sqrt{2}$  we obtain

$$k_y^{\max} = \sqrt{\frac{\sqrt{2} - 1}{2}} k_p \approx 0.455 k_p. \quad (13)$$

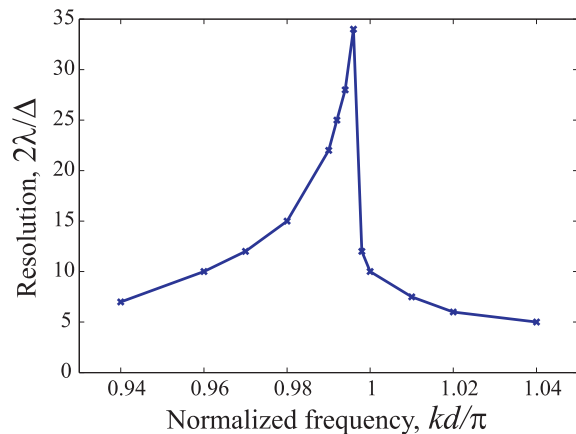


FIG. 8: Normalized resolution  $2\lambda/\Delta$  as a function of the normalized frequency of operation  $kd/\pi$ , for the case of  $k_p d/\pi = 11.3$ .

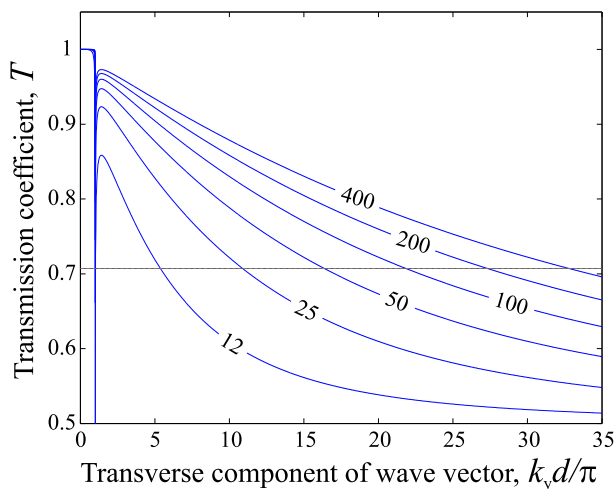


FIG. 9: Dependence of the transmission coefficient  $T$  (absolute value) on transverse component of wave vector  $k_y d/\pi$  for the case when  $kd/\pi = 1$  and various values of plasma frequency  $k_p d/\pi = 12.5 \cdot 2^n$ , where  $n=0,1,2,3,4$ . The numbers at the figure correspond to the values of  $k_p d/\pi$

Thus, the resolution  $\Delta/2$  has the following form:

$$\Delta/2 = \frac{\pi}{0.455k_p} = 1.1\lambda \frac{k}{k_p} = 2.75a \sqrt{\ln \frac{a}{2\pi r} + 0.5275l_{resol}}. \quad (14)$$

Thus, the smaller is the ratio  $k/k_p$  the better is the resolution of the system. Formula  $\hat{resol}$  shows that the resolution of a wire medium lens is only limited by the ability to fabricate very dense arrays of wires, i.e. the limit of resolution only depends ultimately on the value of the lattice constant of the crystal. By decreasing the period of wire medium one can greatly improve resolution of the system. This fact is illustrated in Fig. 9, which shows the transmission characteristic calculated for different values of the plasma frequency. For extremely thin wires and very high frequencies the effect of losses may not be negligible. Nevertheless, at the microwave domain, this effect is expected to be of second order.

## VI. CONCLUSION

In this paper, the resolution of sub-wavelength lenses formed by wire medium has been studied. It was shown that the resolution does not depend on the thickness of the lens, which can in principle be made as thick as required by the application. By slightly tuning the frequency of operation, it is possible to achieve the ultimate limit on resolution dictated by the periodicity of the system (lattice constant of the crystal), even though this regime is very narrow band. The average level of resolution ultimately depends on the period of the lattice. By reducing the lattice constant it may be possible to realize imaging systems with virtually no limit of resolution. This makes the wire medium lens a unique imaging device capable of transmitting distribution of TM-polarized electric field with sub-wavelength resolution at the microwave frequency range.

- 
- [1] P. A. Belov, C. R. Simovski, and P. Ikonen, *Phys. Rev. B* **71**, 193105 (2005).
  - [2] W. Rotman, *IRE Trans. Ant. Propag.* **10**, 82 (1962).
  - [3] J. Brown, *Progress in dielectrics* **2**, 195 (1960).
  - [4] J. Pendry, A. Holden, W. Steward, and I. Youngs, *Phys. Rev. Lett.* **76**, 4773 (1996).
  - [5] P. Belov, R. Marques, S. Maslovski, I. Nefedov, M. Silveirinha, C. Simovski, and S. Tretyakov, *Phys. Rev. B* **67**, 113103 (2003).
  - [6] P. A. Belov, Y. Hao, and S. Sudhakaran, submitted to *Phys. Rev. B*, (arXiv: cond-mat/0508696) (2005).
  - [7] M. Silveirinha, submitted to *IEEE Trans. Antennas. Propagat.* (arxiv: cond-mat/0509612) (2005).
  - [8] T. Wu, *Frequency-selective surface and grid array* (Wiley, NY, 1995).
  - [9] P. Belov, S. Tretyakov, and A. Viitanen, *J. Electromagn. Waves Applic.* **16**, 1153 (2002).
  - [10] V. Agranovich and V. Ginzburg, *Spatial dispersion in crystal optics and the theory of excitons* (Wiley-Interscience, NY, 1966).
  - [11] G. Agarwal, D. Pattanayak, and E. Wolf, *Phys. Rev. B* **10**, 1447 (1974).
  - [12] J. L. Birman and J. J. Sein, *Phys. Rev. B* **6**, 2482 (1972).
  - [13] C. Luo, S. G. Johnson, J. D. Joannopoulos, and J. B. Pendry, *Phys. Rev. B* **68**, 045115 (2003).
  - [14] M. Silveirinha and C. A. Fernandes, *IEEE Trans. on Microwave Theory and Tech.* **51**, 1460 (2003).
  - [15] S. A. Maier, M. L. Brongersma, and H. A. Atwater, *Appl. Phys. Lett.* **78**, 16 (2001).